Preferential Co and Fe atom occupancy in R2(Fe1-xCo)14B intermetallic compounds (R = Nd, Y and Ce)

Gabriel Gomez Eslava, Masaaki Ito, Claire Colin, Masao Yano, Tetsuya Shoji, Akira Kato, Emmanuelle Suard, Nora Dempsey, Dominique Givord

Preferential Co and Fe atom occupancy in $R_2(Fe_{1-x}Co_x)_{14}B$ intermetallic compounds (R = Nd, Y and Ce)

Gabriel Gomez Eslava[a,*], Masaaki Ito[b], Claire V. Colin[a], Masao Yano[b], Tetsuya Shoji[b], Akira Kato[b], Emmanuelle Suard[c], Nora M. Dempsey[a] and Dominique Givord [a,1]

[a]Univ. Grenoble Alpes, Grenoble INP, Institut Néel, 38000 Grenoble, France
[b]Advanced Material Engineering Division, Toyota Motor Corporation, Susono 410-1193, Japan
[c]Institut Laue Langevin - ILL, 38000 Grenoble, France

ARTICLE INFO

Keywords:
Permanent magnets
Preferential site occupancy
Crystal structure
Neutron powder diffraction
Magnetocrystalline anisotropy

Abstract

A powder neutron scattering study of atom substitution in $Nd_2(Fe_{1-x}Co_x)_{14}B$, $Y_2(Fe_{1-x}Co_x)_{14}B$ and $Ce_2(Fe_{1-x}Co_x)_{14}B$ compounds is presented. Compared to previous studies, this one benefits from the considerable progress made in neutron diffraction measurements and their analysis during the last 15 years. The normalization of the occupancy values to those expected from a random distribution permits to reveal small deviations from random distribution. On all crystallographic sites some preferential occupancy is evidenced, the extent of which depends on the Co versus Fe content. A statistical model quantitatively describing site occupancies is proposed, which allows us to study the extreme cases of very dilute substitutions. Steric considerations primarily determine atom substitution, more particularly Fe-substitution in Co-rich compounds. The enthalpy of mixing must also be considered to describe Co preferential occupancies more exactly.

1. Introduction

The best presently known hard magnetic materials are based on $R_2(Fe_{1-x}Co_x)_{14}B$ compounds (R=rare earth). In these compounds the high value of the Fe magnetic moment leads to large spontaneous magnetization ($\mu_0 M_s = 1.61T$ in $Nd_2Fe_{14}B$). The magnetocrystalline anisotropy is dominated by the R atoms, with uniaxial character in compounds in which the R Stevens coefficient α_J is negative (e.g. Nd and Dy). The overall Fe anisotropy is also uniaxial; in $Nd_2Fe_{14}B$ it represents about 20% of the anisotropy field at room temperature ($\mu_0 H_a \approx 8T$). Minor Co substitution for Fe leads to a very significant increase in the Curie temperature. This in turn preserves the R anisotropy up to higher temperature, as required for magnets having sufficient coercivity at the operating temperature of high-performance motors, of the order of 180 degC. The anisotropy in $Y_2Co_{14}B$ has basal plane character, while it is uniaxial in $Y_2Fe_{14}B$ [1]. This suggests that the random introduction of Co atoms should induce a monotonic drop in the 3*d* uniaxial magnetocrystalline anisotropy. Contrary to this, a beneficial increase in magnetocrystalline anisotropy is found in $R_2(Fe_{1-x}Co_x)_{14}B$ alloys in which a minor fraction of Co atoms, up to 30%, is substituted for Fe [1]. This suggests that the distribution of Co atoms over the six different transition metal sites of the $Nd_2(Fe_{1-x}Co_x)_{14}$-type structure does not occur randomly, but rather some preferential site occupancy exists. The analysis of Co preferential atom occupancy in $R_2(Fe_{1-x}Co_x)_{14}B$ compounds has been the subject of various previous studies, using either neutron scattering [2, 3] or Mössbauer spectroscopy [4, 5, 6, 7]. However, there are discrepancies in the preferential occupancy reported in different works. In addition, in most of the cases cited above, the total amount of Co (Fe) atoms substituted for Fe (Co) was determined at each considered alloy composition. Such data suffer from the fact that at low "solute" concentration, the occupancy of each crystallographic site by solute atoms is small by definition and, at high concentration, the occupancy is necessarily close to random. It is much more difficult, but at the same time much more meaningful, to derive the occupancies normalized to those expected for random occupancy. This procedure requires the maximum resolution possible, since for very dilute substitutions it is unavoidable to divide by very small quantities, giving rise to rather large uncertainty values. The considerable progress made in neutron crystallographic studies and their analysis during the last 15 years has stimulated us to undergo a new neutron powder diffraction study of Co-substitution in $Nd_2Fe_{14}B$, $Y_2Fe_{14}B$ and $Ce_2Fe_{14}B$ compounds. This improved precision allows us to propose a diffusion model, based on a probabilistic approach, that describes with outstanding agreement the Fe/Co occupancies, and the preference for Fe and Co atoms at certain sites. This rather general model can be applied to different intermetallic compounds, as no restrictions or approximations concerning the specifics of the material are imposed. Thanks to this model, the preferential occupancy in the limit of very dilute substitution (a few ppm) can be studied in detail.

Here we present the analysis of three different families of compounds, differing in the R atom. As mentioned above, $Nd_2Fe_{14}B$ is the archetype of compounds in this series. In $Y_2Fe_{14}B$, Y being nonmagnetic, the determination of atom preferential occupancy should open the way to reanalyzing the Co-dependent variation of the magnetocrystalline anisotropy, as originally proposed by Hong *et al.* [8]. Finally, recent studies [9, 10, 11] have shown that some Ce may be substituted for Nd in $Nd_2Fe_{14}B$ without deteriorat-

*Corresponding author
ORCID(s): https://orcid.org/0000-0003-1917-8768 (G.G. Eslava)
[1]Deceased author - 4th February 2019.

ing the hard-magnetic properties significantly and the concurrent replacement of a small amount of Fe by Co permits to partially revert the detrimental effect of Ce on the exchange interactions and magnetocrystalline anisotropy. These observations have attracted a specific interest in Ce-based compounds in the series.

2. Experimental protocol and preferential occupancy determination

Samples with overall composition $R_2(Fe_{1-x}Co_x)_{14}B$, (R = Nd, Y, and Ce; $x = 0$, 0.286, 0.5, 0.714, 0.926), were prepared by melt spinning. The obtained ribbons were annealed at 780°C for 24 h, under vacuum ($P \sim 10^{-7}$ mbar) and then crushed into powder, of about 50 μm particle diameter. The final composition of the samples was confirmed by the Inductively Coupled Plasma (ICP) technique. For all Nd based samples the formation of the 2:14:1 phase was confirmed by X-ray diffraction (XRD), while a minor amount of Laves phase $Nd(Fe,Co)_2$ was detected in samples with $x \geq 0.5$. In Fe-rich Y samples the 2:14:1 phase was also the major phase, and the presence of a small fraction of the $Y(Fe,Co)_2$ Laves phase was detected already for $x = 0.286$. In all the above cases the volume fraction of Laves phase was estimated to be less than 1%. For the Y sample with $x = 0.714$, a significant fraction of the $Y_2(Fe,Co)_{17}$ phase was identified, and it was the main phase for $x = 0.926$. In Ce compounds, only two samples presented the desired structure, those with $x = 0$ and 0.286. According to literature the upper solubility limit for Co in $Ce_2(Fe_{1-x}Co_x)_{14}B$ is less than $x = 0.4$ [12, 13].

Neutron powder diffraction (NPD) measurements were performed at 300 K on the D2B beamline at the ILL (Grenoble, France) [14]. Approximately 1g of powder of each sample was introduced into a 6mm-diameter vanadium cylinder. D2B is a high-resolution diffractometer with a very high take-off angle (135°) [15]. The selected neutron wavelength was $\lambda = 1.594$Å, corresponding to the (335) Bragg reflection of a germanium vertically focusing monochromator. The collimation was set to 10'. On this instrument, detection is realized using a multidetector having a horizontal aperture of 200 mm. A complete diffraction pattern is obtained after about 25 steps of 0.05° in 2θ, since the 128 3He counting tubes are spaced at 1.25° intervals. Such scans take typically 30 minutes and were repeated to improve statistics. In this study, collection of one pattern typically required 3 hours.

All the experimental patterns are shown in the supplementary material, in Figures SM1 for Nd compounds and SM2 for Y and Ce compounds. The total intensities in Co rich samples are around four times lower than those for Fe rich samples. This is related to the high scattering length of Fe (9.45 fm) compared to Co (2.49 fm). At room temperature all the compounds are ferromagnetic. As the periodicity of the magnetic lattice is the same as the nuclear one, the magnetic reflections are superimposed on nuclear ones, and their contributions to Bragg peaks must be evaluated. In $Nd_2Fe_{14}B$ and $Y_2Fe_{14}B$, the Fe magnetic moment on each transition metal (TM) site was deduced from a polarized neutron study of this compound, performed at 4.2 K and 250 K [16]. The moment values in $Y_2Fe_{14}B$ at 300 K on each crystallographic site, were calculated assuming that all the individual magnetic moments evolve with temperature as the spontaneous magnetization does. The temperature dependence of the spontaneous magnetization in $Y_2Fe_{14}B$ was taken from Bolzoni *et al.* [17]. In the case of $Nd_2Fe_{14}B$, the Nd moment at 300 K was calculated using the model described by Cadogan *et al.* [18], using the same exchange and Crystalline Electric Field parameters reported by the authors. The low temperature ratio between Fe moments in this compound and in $Y_2Fe_{14}B$, derived from Bolzoni *et al.* [17], was assumed to be temperature independent, thus permitting the Fe moments at 300 K on all crystallographic sites to be calculated from the moments in $Y_2Fe_{14}B$ at the same temperature. In $Ce_2Fe_{14}B$, the Fe moment values on the different sites at 300 K were obtained from the values in $Y_2Fe_{14}B$, multiplied by a coefficient equal to the ratio of the spontaneous magnetization in these two compounds at that temperature.

No complete information about the evolution of individual moments as a function of Co content was found in the literature. However, Huang *et al.* [19], showed that a similar Co-dependence of M_s is observed in different $R_2(Fe_{1-x}Co_x)_{14}B$ compounds (R = Y, Nd and Gd), with a maximum at $x \approx 0.15$. According to this, we assumed in the refinement procedure that all TM moments evolve with Co concentration in the same way as the spontaneous magnetization of $Y_2(Fe_{1-x}Co_x)_{14}B$ does. For each TM crystallographic site, a unique magnetic moment was assigned. Almost all the compounds in this study are known to have uniaxial character and thus the magnetic moments were assumed to be aligned along the c-axis. The only exception is the sample $Y_2(Fe_{0.286}Co_{0.714})_{14}B$, for which the magnetic moments were assumed to be along the *a*-axis (basal plane anisotropy). All the individual magnetic moments of $R_2Fe_{14}B$ compounds used for the refinements are presented in Table SM1 of the supplementary material. The reduction factor of these moments as a function of Co content are presented in Table SM2.

The NPD data were analyzed using the FullProf software, based on the Rietveld refinement method [20]. The initial values of the parameters describing the $Nd_2(Fe_{1-x}Co_x)_{14}B$-type crystallographic structure of all compounds were taken from the literature [21]. For Co doped samples, we initially assumed that Co is randomly distributed over the six TM sites, according to its nominal content x. Two constraints were imposed on the occupancy factors: (i) the total amount of each type of atom respects the alloy composition and (ii) the total occupancy of each site is equal to one (fully occupied sites).

The experimental diagrams, together with the results of Rietveld analysis for all the samples presenting the $R_2(Fe_{1-x}Co_x)_{14}B$ phase are shown in Fig. SM1 (Nd compounds) and SM2 (Y and Ce compounds) of the supplementary material. In general, the agreement between experimen-

tal and calculated patterns is excellent; the conventional reliability factors of the crystal structure (R_{Bragg} and R_F), for the magnetic structure (R_M) and the global parameter χ^2, as defined elsewhere, are listed in table SM3.

The above reliability factors were systematically compared to those obtained when a random distribution over all TM sites is imposed (see Fig. SM3 and Table SM3). In all cases, their values are lower when preferential occupancy is allowed. The convergence of occupancy values was also tested by repeated refinements, each time giving randomly chosen initial occupancy values, respecting the two constraints described above. For all samples the difference between consecutive refinements is smaller than the statistical error given by the software. The refined Co occupancy factors for all compounds are listed in Table 1. All other refined parameters are listed in Tables SM4 to SM6. The errors indicated in these tables are the statistical errors provided by the FullProf software, corrected for parameter correlation ("SCor" parameter). Note that the error bars corresponding to the Y sample with $x = 0.714$ are much larger than for all the other samples, reflecting the presence of a significant secondary phase, as mentioned above.

The variations of the lattice parameters a and c for the three series of compounds are plotted as a function of x in Fig. SM4. The corresponding c/a ratio and cell volume are plotted in fig SM5. As x increases, a monotonous decrease of the lattice parameters and cell volume is observed. This simply represents the fact that the metallic radius of Co is lower than that of Fe.

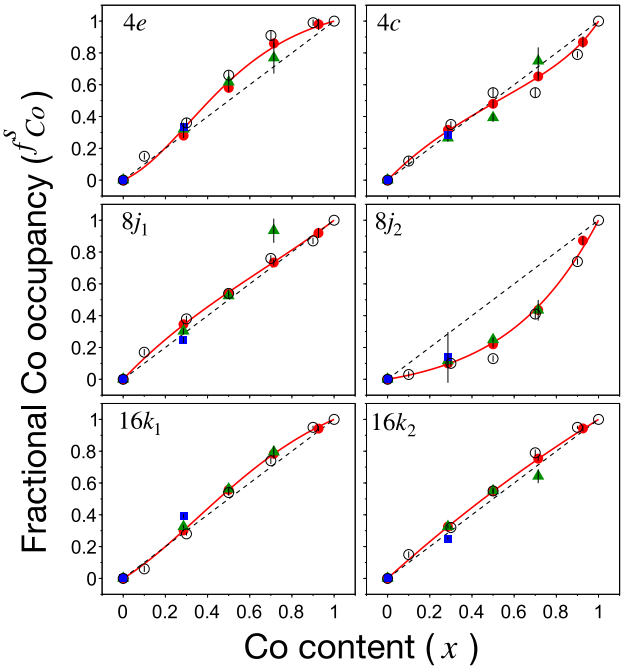

Figure 1: Co fractional occupancies, f^s_{Co}, on the different TM sites as a function the Co concentration for $R_2(Fe_{1-x}Co_x)_{14}B$. Solid circles in red: Nd compounds. Green triangles: Y compounds. Blue squares: Ce compounds. Open circles from Herbst *et al.* [2]. Solid lines in red are the result of calculated occupancies (see section 4). Dashed straight lines represent random occupancy.

3. Peferential occupancy analysis

Fig. 3 shows the fractional Co occupancy as a function of Co content, $f^s_{Co}(x)$, over the six TM crystallographic sites, for the three considered families of compounds. Solid symbols represent our results, whereas open symbols correspond to those of Herbst *et al.* [2] The dashed lines in the graphs represent the hypothetical case of random distribution of Co among the different TM sites. As can be seen, some deviation from random occupancy is observed on all sites. The more dramatic case is for site $8j_2$, which is strongly under-occupied by Co. Although used classically [2, 3, 4, 5, 6], Fig. 1 does not represent an optimum presentation of the experimental results. The occupancies normalized to those expected for random distribution (f^s_{Co}/x for Co and $f^s_{Fe}/(1-x)$ for Fe) are much more significant. These are shown in Fig. 2 for Nd compounds and Fig. 3 for Y and Ce compounds (only $Ce_2(Fe_{1-x}Co_x)_{14}B$ with x = 0.286). In both figures, in the left-hand side column we present f^s_{Co}/x and in the right-hand side column $f^s_{Fe}/(1-x)$. Note that the normalization procedure used to obtain these plots requires sufficient data accuracy, so that the error bars do not become exceedingly high after division by (small) x or $(1-x)$. As seen in the figures, the relative error bars remain below 10 % for most of the presented data. Compared to $Nd_2(Fe_{1-x}Co_x)_{14}B$ data collected in the present study, on a modern high-flux neutron diffractometer, Herbst *et al.* data [2] (open circles in Fig. 2) are more scattered. This can be ascribed to the fact that their accuracy is less, as expected. From a Mössbauer study on very dilute ^{57}Co-doped $Nd_2Fe_{14}B$ compounds (^{57}Co content $\approx$ 1 ppm), Liao *et al.* [7] derived Co occupancies normalized to random, shown in Fig. 2 as open diamonds. For the two $16k$ sites and the two $8j$ sites, the agreement with the present data is excellent. However, it is not as good for the less occupied $4c$ and $4e$ sites.

4. Modelling preferential occupancy

4.1. Model concept

With a view to accounting for the different experimental occupancies, by either Fe or Co, of the TM sites in the $R_2(Fe_{1-x}Co_x)_{14}B$ crystal structure, we developed a simple statistical model. Each sample of chemical composition $R_2(Fe_{1-x}Co_x)_{14}B$, is characterized by the already defined relative contents x of Co and $(1-x)$ of Fe. Under certain experimental conditions, the TM atoms have the possibility of interdiffusing between different sites in the crystal. The atoms jump from one position to another thanks to the presence of vacancies. We are interested in double jumps that leave the number of atoms on a given crystallographic site invariant. Double jumps leading to the replacement of an Fe atom by Co and vice versa may occur with different probabilities, representing the different "attractiveness" of each site for either Co or Fe atoms. Via such processes, the sys-

Table 1
Fractional Co site occupancies f^s_{Co} as a function of the Co content x, in $R_2(Fe_{1-x}Co_x)_{14}B$ compounds

x	$4e$	$4c$	$8j_1$	$8j_2$	$16k_1$	$16k_2$
			R = Nd			
0	0	0	0	0	0	0
0.286	0.280(11)	0.316(11)	0.346(11)	0.100(11)	0.302(6)	0.326(6)
0.5	0.580(26)	0.480(26)	0.538(17)	0.220(20)	0.557(11)	0.549(12)
0.714	0.860(26)	0.652(26)	0.734(20)	0.436(16)	0.784(13)	0.753(13)
0.926	0.980(36)	0.868(36)	0.920(32)	0.872(28)	0.942(17)	0.943(18)
			R = Y			
0	0	0	0	0	0	0
0.286	0.320(22)	0.264(22)	0.302(19)	0.116(19)	0.325(11)	0.325(11)
0.5	0.616(19)	0.392(25)	0.524(19)	0.248(16)	0.561(11)	0.550(11)
0.714	0.768(98)	0.748(87)	0.934(76)	0.434(65)	0.794(38)	0.642(46)
			R = Ce			
0	0	0	0	0	0	0
0.286	0.332(26)	0.286(20)	0.246(20)	0.138(16)	0.393(11)	0.251(11)

tem evolves from any assumed initial situation towards an equilibrium situation, characterized by a certain preferential occupancy of the TM sites. To analyze the occupancy of a given crystallographic site s, we arbitrarily assume that the other five TM sites form together a unique hypothetical site, designated by t. Within an elementary time interval dt, the probability of a Co atom jumping from site t to site s is defined as $P^{ts}_{Co} = p^{ts}_{Co}dt$, and from site s to site t, the probability is $P^{st}_{Co} = p^{st}_{Co}dt$, where p^{ts}_{Co} and p^{st}_{Co} are proportional to diffusion rate constants. The probability ratio $r^s_{Co} = (P^{ts}_{Co})/(P^{st}_{Co})$ represents how much Co atoms prefer the s site with respect to the t site. We label this the affinity of Co atoms for site s. For $r^s_{Co} > 1$, Co atoms are attracted towards s, and for $r^s_{Co} < 1$ they are attracted towards t. One defines similarly the probabilities for Fe atoms as P^{ts}_{Fe} and P^{st}_{Fe}. The probability ratio $r^s_{Fe} = (P^{ts}_{Fe}/(P^{st}_{Fe})$ describes Fe affinity towards s sites. An important parameter in the analysis is the ratio between Co and Fe affinities on site s, called the affinity ratio, defined as:

$$r_s = \frac{r^s_{Co}}{r^s_{Fe}} \tag{1}$$

The occupancies normalized to random of the two sites s and t by either Co or Fe can be written as:

$$f^s_{Co}/x = (1 - \delta^s_{Co}) \tag{2a}$$
$$f^s_{Fe}/(1-x) = (1 + \delta^s_{Fe}) \tag{2b}$$
$$f^t_{Co}/x = (1 + \delta^t_{Co}) \tag{2c}$$
$$f^t_{Fe}/(1-x) = (1 - \delta^t_{Fe}) \tag{2d}$$

where δ^s_{Co}, δ^s_{Fe}, δ^t_{Co} and δ^t_{Fe} represent deviations from random occupancy. Note that for random occupancy these quantities are equal to zero and the occupancies, normalized to random, are identical to 1. The condition that the total occupancy of each site must be equal to 1 leads to:

$$\delta^s_{Fe} = \delta^s_{Co}x/(1-x) \tag{3a}$$
$$\delta^t_{Fe} = \delta^t_{Co}x/(1-x) \tag{3b}$$

The condition that the sum of the occupancies of a given type of atom must be equal to its content in the alloy leads to:

$$\delta^t_{Co} = \delta^s_{Co}(n_s/n_t) \tag{4a}$$
$$\delta^t_{Fe} = \delta^s_{Fe}(n_s/n_t) \tag{4b}$$

where n_s and n_t are the multiplicities of sites s and t, respectively (see Tab. 1). Assume that the distribution of atoms on the different crystallographic sites deviates from equilibrium distribution. The associated elementary variation in Co occupancy on site s, δ^s_{Co}, due to atom exchange, is equal to the probability of an Fe atom being replaced by Co, minus the probability of a Co atom being replaced by Fe:

$$\delta f^s_{Co} = n_s n_t (f^t_{Co} f^s_{Fe} P^{ts}_{Co} P^{st}_{Fe} - f^t_{Fe} f^s_{Co} P^{ts}_{Fe} P^{st}_{Co}) \tag{5}$$

With the above defined affinities, r^s_{Fe} and r^s_{Co}, and affinity ratio, r_s, and assuming for simplicity that $P^{ts}_{Co} = P^{st}_{Fe}$, expression (5) reduces to:

$$\begin{aligned} \delta f^s_{Co} &= n_s n_t (f^t_{Co} f^s_{Fe} r^s_{Co} P^{ts}_{Co} - f^t_{Fe} f^s_{Co} r^s_{Fe} P^{st}_{Fe}) \\ &= n_s n_t P^{ts}_{Co} r^s_{Fe} (f^t_{Co} f^s_{Fe} r_s - f^t_{Fe} f^s_{Co}) \end{aligned} \tag{6}$$

We are interested in the equilibrium situation, when $\delta^s_{Co} = 0$. By imposing this condition and replacing the fractional occupancies by their expressions (2a) to (2d), one arrives at:

Table 2
Co over Fe affinity ratio, r_s, in Fe-rich compounds ($x \to 0$) and Co-rich compounds ($x \to 1$), for R = Nd and Y. In the last four columns we list the Voronoi (site) volumes calculated from refined atomic positions of the same compounds, in the limits ($x \to 0$) and ($x \to 1$).

	Affinity ratio, r_s				Voronoi volume(Å^3)			
	Nd		Y		Nd		Y	
site	$x \to 0$	$x \to 1$	$x \to 0$	$x \to 1$	$x \to 0$	$x \to 1$	$x \to 0$	$x \to 1$
$4e$	0.58	2.80	0.58	2.80	11.73	10.78	11.69	10.81
$4c$	1.40	0.45	1.00	0.40	12.33	11.78	12.13	11.56
$8j_1$	1.50	1.00	1.10	1.05	12.25	11.60	12.17	11.52
$8j_2$	0.20	0.30	0.25	0.31	12.72	11.88	12.58	11.75
$16k_1$	0.75	2.00	0.80	2.35	11.81	10.97	11.69	10.94
$16k_2$	1.30	1.30	1.50	1.11	11.60	10.85	11.45	10.89

$$\left(1+\delta^s_{Co}\frac{n_s}{n_t}\right)\left[1+\delta^s_{Co}\left(\frac{x}{1-x}\right)\right]r_s = \left[1-\delta^s_{Co}\frac{n_s}{n_t}\left(\frac{x}{1-x}\right)\right](1-\delta^s_{Co}) \quad (7)$$

For a given compound, characterized by the value of x, this expression, quadratic in δ^s_{Co}, depends only on the affinity ratio r_s. All other occupancies are simple functions of δ^s_{Co} (see expressions (3) and (4) above). Note that in the limit $x \to 0$, one has:

$$\lim_{x\to 0}\delta^s_{Co} = \frac{(1-r_s)}{1+r_s(n_s/n_t)} \quad (8)$$

together with $\delta^s_{Fe} \to 0$. Reciprocally, in the limit $x \to 1$:

$$\lim_{x\to 1}\delta^s_{Fe} = \frac{1-r_s}{r_s+(n_s/n_t)} \quad (9)$$

together with $\delta^s_{Co} \to 0$. These two limit situations represent the case of very dilute substitutions.

4.2. Application of model to $R_2(Fe_{1-x}Co_x)_{14}B$ compounds

For each considered compound, the value of r_s is derived by solving equation (7), for normalized occupancies equal to experimental ones. Across a given series, defined by the nature of the R element, it is not possible with a unique value of r_s to account for the experimental variation of the site occupancies, in the whole concentration range from $x = 0$ to $x = 1$. Whereas a monotonous deviation from random occupancies at each site would happen if r_s was a constant, the experimental deviations present, on various sites, a maximum or a minimum at intermediate x values (see Fig. 3). This suggests expressing the affinity ratio as a function of the relative content of Fe and Co in the compounds:

$$r_s(x) = (1-x)r_{s_{(x\to 0)}} + x r_{s_{(x\to 1)}} \quad (10)$$

where $r_{s(x\to 0)}$ and $r_{s(x\to 1)}$ are affinity ratio values accounting for the occupancies in Fe-rich compounds and Co-rich compounds, respectively. With this unique additional hypothesis, a very satisfactory description of all experimental data is obtained (see continuous lines in Fig. 3, 2 and 3). The obtained values of $r_s(x \to 0)$ and $r_s(x \to 1)$ are listed in Table 2 for Nd and Y compounds. Very similar results are obtained for the Nd and Y based systems, as seen by comparing both continuous curves in Fig. 3. In the case of the $4e$ site, the calculated curves coincide since the same affinity ratios are used for both systems.

5. Discussion

Three physical parameters are expected to govern preferential site occupancies in compounds with two different atoms (here Fe and Co) sharing the same crystallographic sites. The first of these is the volume effect, favoring the occupancy of large atomic sites by bigger atoms (Fe in the present case). The second is the enthalpy of mixing. The enthalpy of formation of R-Co compounds is in general lower than that of R-Fe compounds [22] and this favors Co atoms on sites with a large number of R neighbors. Reciprocally, the enthalpy of formation of Fe_2B is lower than that of Co_2B [23] and one may expect Fe atoms to prefer sites with B neighbors. The last term is the entropy, which favors mixing between different atoms. Calculated Co and Fe occupancies at the limits $x \to 0$ and $x \to 1$, derived from expressions (8) and (9), are plotted in Fig. 4 as a function of the Voronoi (site) volume (see Table 2). The latter were calculated using the DIDO-95 software [24] from the refined atomic positions of $Nd_2Fe_{14}B$, $Y_2Fe_{14}B$ and $Nd_2(Fe_{0.074}Co_{0.926})_{14}B$. For $Y_2Co_{14}B$, the atomic positions were taken from literature [25]. In these figures, a point above 1 (shaded area) means over-occupancy with respect to random and below 1 means under-occupancy. Such plots aim at revealing volume effects in site occupancies. Assuming that site occupancy is a linear function of the site volume, the normalized occupancy of site s by Co atoms in the limit $x \to 0$ should follow

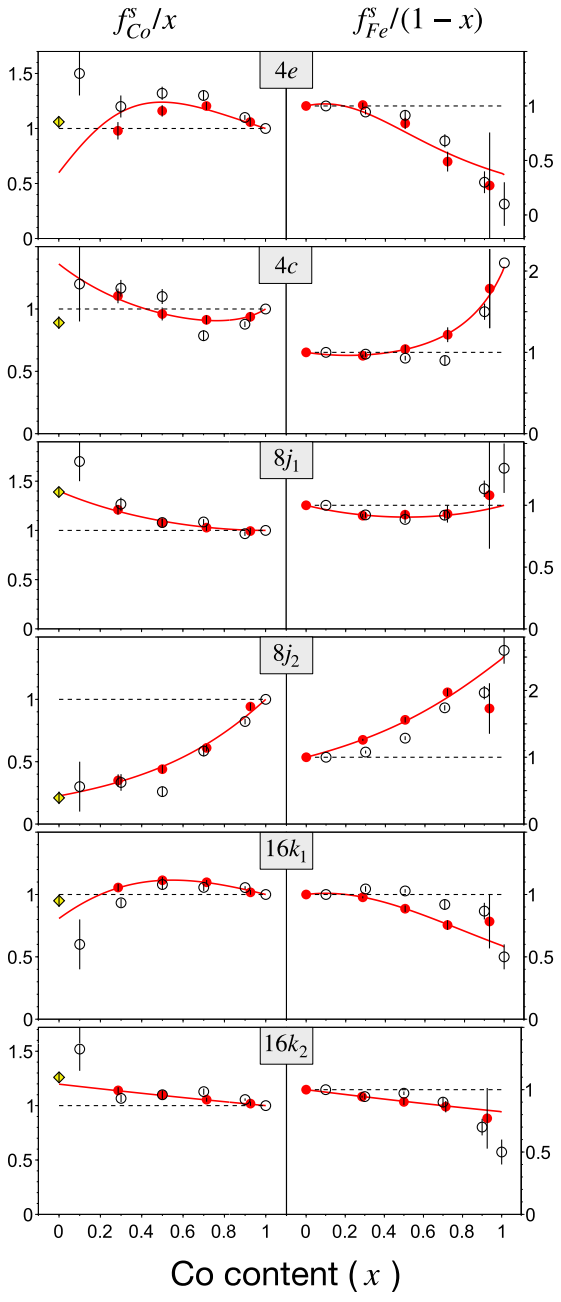

Figure 2: Co (left) and Fe (right) occupancies, normalized to random, in $Nd_2(Fe_{1-x}Co_x)_{14}B$. From top to bottom: sites $4e$, $4c$, $8j_1$, $8j_2$, $16k_1$ and $16k_2$. Solid circles (red): present data; open circles: data from Herbst *et al.* [2]; Yellow diamonds: data from Liao *et al.* [7]. Continuous red lines: calculated Fe and Co occupancies (see Section 4). Random occupancy is represented by the straight dashed black lines.

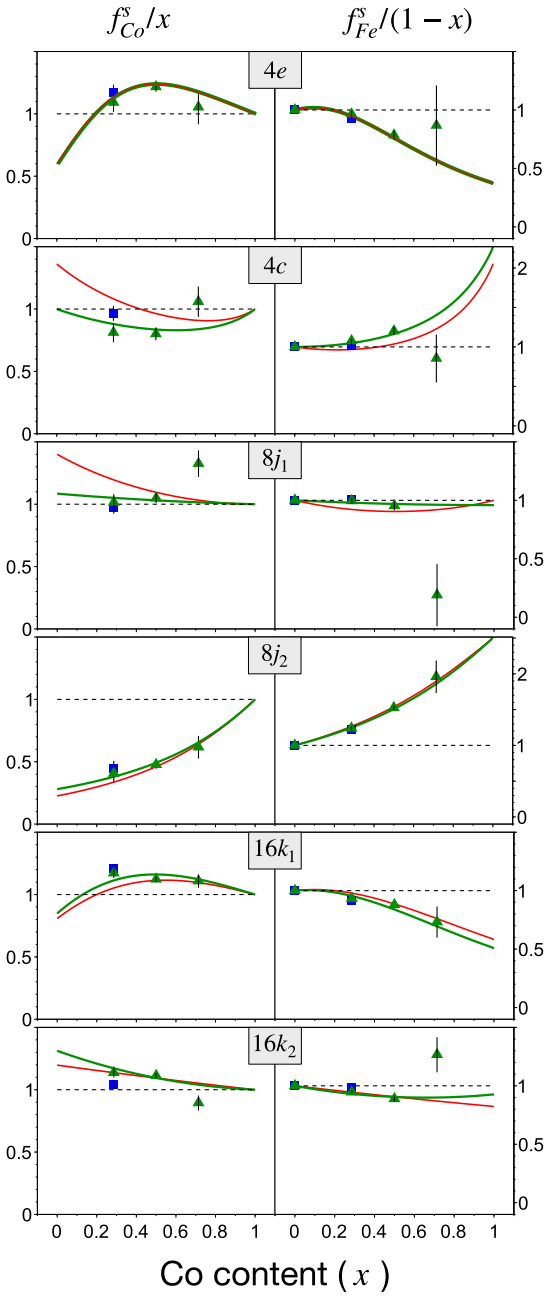

Figure 3: Co (left) and Fe (right) occupancies, normalized to random, in $Y_2(Fe_{1-x}Co_x)_{14}B$, $x = 0$, 0.286, 0.5 and 0.714 (green triangles) and $Ce_2(Fe_{1-x}Co_x)_{14}B$, $x = 0$ and 0.286 (blue squares). From top to bottom: sites $4e$, $4c$, $8j_1$, $8j_2$, $16k_1$ and $16k_2$. Continuous green curves: calculated Fe and Co occupancies for y compounds(see Section 4). Continous red curves: calculations for Nd compounds (see Fig. 2). The straight dashed black lines represent random occupancy.

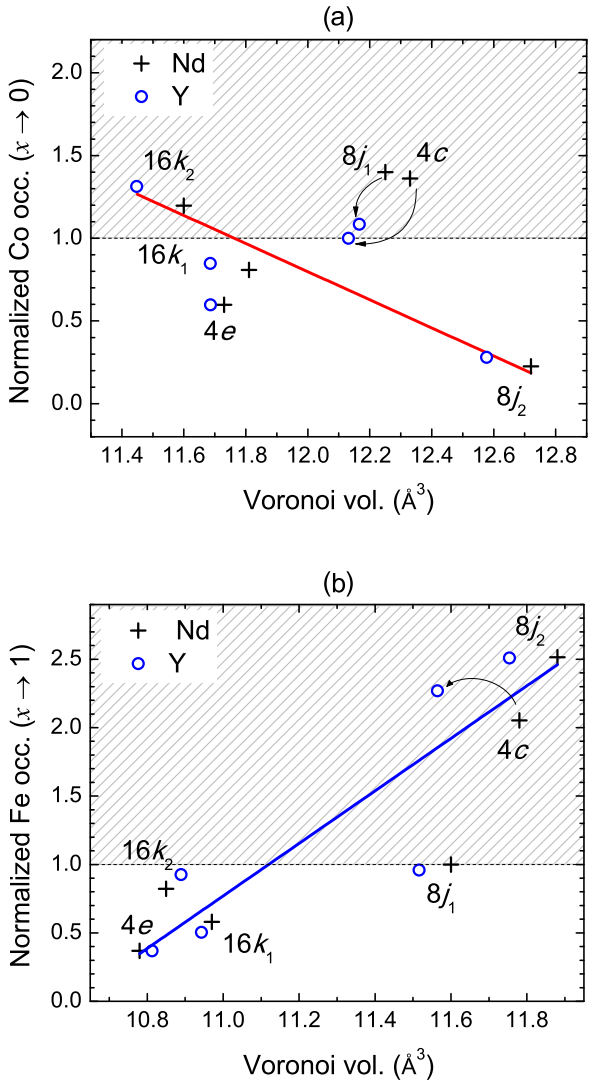

Figure 4: (a) Co normalized occupancy on Fe-rich compounds ($x \to 0$). (b) Fe normalized occupancies in Co-rich compounds ($x \to 1$). The solid lines represent linear dependency of occupancy as function of the site volume (Eq. (11) and (12)). Atom occupancies in Nd compounds are represented by "+" symbols and open circles are used for Y compounds.

the expression:

$$f^s_{Co}/x = \alpha_{Co} * V^{Fe}_s + \beta_{Co} \tag{11}$$

where α_{Co} and β_{Co} are phenomenological parameters, and V^s_{Fe} is the Voronoi volume of site s, in the limit $x \to 0$ (see Table 2). Similarly, in Co-rich compounds, the normalized occupancy by Fe atoms should follow:

$$f^s_{Fe}/(1-x) = \alpha_{Fe} * V^{Co}_s + \beta_{Fe} \tag{12}$$

where V^s_{Co} is the Voronoi volume in the limit $x \to 1$. The total occupancy should normalize to 1, given by summation over all sites:

$$\sum_s \frac{n_s}{56}\left(\frac{f^s_{Co}}{x}\right) = 1 \tag{13}$$

and

$$\sum_s \frac{n_s}{56}\left(\frac{f^s_{Fe}}{1-x}\right) = 1 \tag{14}$$

with 56 being the total number of TM sites per unit cell. From (11) and (13), one derives:

$$\beta_{Co} = 1 - \frac{\alpha_{Co}}{56}\sum_s n_s V^{Fe}_s \tag{15}$$

And from (12) and (14):

$$\beta_{Fe} = -\frac{\alpha_{Fe}}{56}\sum_s n_s V^{Co}_s \tag{16}$$

Thus, expressions (11) and (12) depend on a unique parameter, α_{Co} or α_{Fe}.

For Co and Fe occupancies, we determined the α_{Co} and α_{Fe} parameters providing best account of experimental data. Equations (11) and (12) are represented as red and blue lines in and Fig. 4a rand 4b, respectively. The $8j_2$ site is over-occupied by Fe atoms (Fig. 4b) and under-occupied by Co ones (Fig. 4a). The inverse, but to a lesser extent, is found for the $16k_2$ site, which is over-occupied by Co atoms and under-occupied by Fe ones. The occupancies of these two sites do not deviate strongly from the red and blue lines in Fig. 4, i.e., to first approximation, the occupancy of these sites is determined by volume effects. The Co occupancy of site $8j_1$ is well above the red line in Fig. 4a and Fe occupancy is below the blue line in Fig.4b. The environment of this site is rich in R atoms, as shown in Table 3.

As the enthalpy of R-Co alloys is significantly lower than that of R-Fe alloys, the occupancy of this site by Co atoms is favored. The same argument accounts for the strong over-occupancy of site 4*c* by Co atoms in Fig. 4a. Notice that these two crystallographic sites are in fact the most affected by replacing Nd for Y. Unexpectedly, the 4*c* site is (slightly) over occupied by Fe atoms in Co-rich compounds (Fig.4b). This effect may be attributed to the differences in enthalpy occurring when a given atom, Co for instance, is introduced in an Fe-rich or Co-rich compound. In the former case, almost no Co-R bonds are yet formed and $3d-5d$ hybridization may develop. In the latter case, there are already many Co atoms forming bonds with R in the environment, lowering the number of 5*d* electrons available for $3d-5d$ hybridization. In Co-rich compounds (Fig. 4b), the 4*e* and $16k_1$ sites are under-occupied by Fe atoms. This result is expected, considering that the environment of these two sites is poor in R atoms and contains B atoms (see Table 3). However, unexpectedly, these two sites are under-occupied by Co atoms in Fe-rich alloys. The very same arguments used above to explain the over occupancy of the 4*c* sites by Fe atoms may be proposed.

We thus provide a simple method to properly describe the preferential occupancy of TM sites as a function of the Co content. Other studies of $(Dy,Nd)_2Fe_{14}B$ [26], $(La,Ce)_2Fe_{14}B$ and $(La,Nd)_2Fe_{14}B$ [10] compounds have shown that preferential occupancy also occurs in R sites. Furthermore, in reference [26] the authors compare results

Table 3
Coordination number of rare-earth (R), transition metal (TM) and B atoms in the local environment of the different TM sites in $R_2Fe_{14}B$ structure

TM site	Coordination numbers			
	(R)	(TM)	(B)	Total
$4e$	2	9	2	13
$4c$	4	8	0	12
$8j_1$	3	9	0	12
$8j_2$	2	12	0	14
$16k_1$	2	10	1	13
$16k_2$	2	10	0	12

of NPD with ab initio and thermodynamic (CALPHAD) calculations, in order to predict the preference of Dy to occupy certain R sites. Other authors [27] use molecular dynamics in order to calculate preferential occupancy of Ti in $RFe_{1-y}Ti_y$ compounds and are able to predict the preference of Ti to occupy one out of the three available TM sites (8i sites), as confirmed by experiments. It is important to remark that $NdFe_{12}$-based compounds present a rather simple crystal structure (24 atoms/unit cell) compared to the present case of NdFeB-based compounds (68 atoms/unit cell). As the molecular dynamics method is very time consuming, it would take excessively large times to calculate Co occupancy in $R_2TM_{14}B$ compounds. Compared to the abovementioned methods to describe preferential occupancy, our approach is different and unique. Our model is not able to predict site occupancy from first principles, but once affinity ratios are determined, it provides us with a reliable way to calculate the occupancy of a given site for any arbitrary composition, in particular for very diluted cases with ($x \to 0$) and ($x \to 1$). From such calculations we draw physical conclusions regarding preferential occupancy, as discussed above. Notice that the assumptions of our model are not specific of a $R_2TM_{14}B$-type structure, hence it can be applied to the study of preferential occupancy in other R-TM intermetallics.

6. Conclusions

We have performed a high-resolution neutron diffraction study on atom substitution in $R_2(Fe_{1-x}Co_x)_{14}B$ compounds. Some Fe/Co preferential occupancy was observed in all the crystallographic sites, which is better revealed when occupancies normalized to random are taken into account, rather than fractional occupancies. We have demonstrated that the preferential occupancy depends on the Co concentration. A statistical model was developed, quantitively accounting for the preferential occupancies. This allowed us to study two extreme cases: (i) very dilute Co in $Nd_2Fe_{14}B$ and (ii) very dilute Fe in $Nd_2Co_{14}B$. The results are discussed in light of local site environments, taking into account site volume (steric considerations) and the nature of the first neighbors. Steric considerations primarily determine atom substitution, more particularly Fe-substitution in Co-rich compounds. Enthalpy of mixing and entropy considerations must also be considered to describe Co preferential occupancy more exactly in Fe-rich compounds. The results for Ce compounds are similar to those of Y compounds, in agreement with the screened magnetic moment in the former. Individual contributions to total anisotropy coming from Fe and Co in each site should be studied in terms of preferential occupancy.

Acknowledgements: This study is based on results obtained from the future pioneering program "Development of magnetic material technology for high-efficiency motors" (MagHEM), grant number JPNP14015, commissioned by the New Energy and Industrial Technology Development Organization (NEDO).

References

[1] T. Ukai, K. Yamaki, H. Takahashi, N. Mori. *Anisotropy energy of $Y_2Fe_{14}B$, $Y_2Co_{14}B$, $Y_2Fe_{14-x}Co_xB$, and $La_2Co_{14}B$.* J. App. Phys. 69, 4662 (1991).

[2] J. F. Herbst, W. Yelon. *Preferential site occupation and magnetic structure of $Nd_2(Co_xFe_{1-x})_{14}B$ systems.* J. App. Phys. 60, 4224 (1986).

[3] K. Girgis, M. Kraft, U. Weis, P. Fischer, M. Sostarich. *Crystal and magnetic structure of the permanent magnet materials $Nd_2Fe_{14-x}Co_xB$ ($x = 0-14$).* J. Less-Common Met. 162, 335 (1990).

[4] H. M. van Noort, K. H. J. Buschow. *On the site preference of 3d atoms in compounds of the $R_2(Co_{1-y}\ Fe_y\ )_14B$ type*. J. Less-Common Met. 113, L9 (1985).

[5] P. Deppe, M. Rosenberg, S. Hirosawa. *A ^{57}Fe Mossbauer study of $Nd2(Fe_{1-x}Co_x)14B$*. M. Sagawa, J. App. Phys. 61, 4337 (1987).

[6] Y. Sano, H. Onodera, H. Yamauchi, H. Yamamoto. *Magnetic properties of the 3d sublattice in pseudoternary compounds $Y_2(Fe_{1-x}M_x)_{14}B$ with M = Co and Mn.* J. Magn. Magn. Mater. 79, 67 (1989).

[7] L.X. Liao, Z. Altounian, D.H. Ryan. *Cobalt site preferences in iron rare-earth-based compounds*. Phys. Rev. B 47, 11230 (1993).

[8] N. M. Hong, J. J. M. Franse, N. P. Thuy. *Magnetic anisotropy of the $Y_2(Co_{1-x}Fe_x)_{14}B$ intermetallic compounds*. J. Less-Common Met. 155, 151 (1989).

[9] K. P. Skokov, O. Gutfleisch. *Heavy rare earth free, free rare earth and rare earth free magnets – Vision and reality*. Scripta Materialia 154, 289 (2018).

[10] C.V. Colin, M. Ito, M. Yano, N. M. Dempsey, E. Suard, D. Givord. *Solid-solution stability and preferential site-occupancy in (R-R')$_2Fe_{14}B$ compounds*. Appl. Phys. Lett. 108, 242415 (2016).

[11] A. Alam, and D. D. Johnson, *Mixed valency and site-preference chemistry for cerium and its compounds: A predictive density-functional theory study*. Phys. Rev. B 89, 235126 (2014).

[12] E. J. Skoug, M. S. Meyer, F. E. Pinkerton, M. M. Tessema, D. Haddad, J. F. Herbst. *Crystal structure and magnetic properties of $Ce_2(Fe_{1-x}Co_x)_{14}B$ alloys*. J. Alloys Compd. 574, 552 (2013).

[13] T. Wang, D. Kevorkov, M. Medraj. *Phase equilibria and magnetic phases in the Ce-Fe-Co-B system*. Materials 10, 16 (2017).

[14] G. G. Eslava, C. V. Colin, N. M. Dempsey, D. Givord, M. Ito, E. Suard. *Search for preferential site occupancy of Co in $R_2(Fe-Co)_{14}B$ compounds*. Institut Laue-Langevin (ILL) doi:10.5291/ILL-DATA.5-23-691 (2017).

[15] https://www.ill.eu/users/instruments/instruments-list/d2b/characteristics/

[16] D. Givord, H. S. Li, F. Tasset. *Polarized neutron study of the compounds $Y_2Fe_{14}B$ and $Nd_2Fe_{14}B$*. J. App. Phys. 57, 4100 (1985).

[17] F. Bolzoni, J. P. Gavigan, D. Givord, H. S. Li, O. Moze, L. Pareti. 3*d magnetism in $R_2Fe_{14}B$ compounds*. J. Magn. Magn. Mater. 66, 158 (1987).

[18] J. M. Cadogan, J. P. Gavigan, D. Givord, H.S. Li. *A new approach to the analysis of magnetisation measurements in rare-earth/transition-metal compounds: application to $Nd_2Fe_{14}B$*. J. Phys. F: Met. Phys. 18, 779 (1988).

[19] M. Q. Huang, E. B. Boltich, W. E. Wallace. *Magnetic characteristics of $R_2(Fe,Co)_{14}B$ systems (R=Y, Nd and Gd)*. J. Magn. Magn. Mater. 60, 270 (1986).

[20] J. Rodriguez-Carvajal. *Recent advances in magnetic structure determination by neutron powder diffraction*. Physica B 192, 55 (1993).

[21] J. F. Herbst, J. J. Croat, F. E. Pinkerton, W. B. Yelon. *Relationships between crystal structure and magnetic properties in $Nd_2Fe_{14}B$*. Phys. Rev. B 29, 4176(R) (1984).

[22] G. H. Rao, S. Wu, X. H. Yan, Y. L. Zhang, W. H. Tang, J. K. Liang. *Enthalpies of formation of rare earth-3d metal alloys and intermetallic compounds*. J. Alloys Compd. 202, 101 (1993).

[23] S. Sato, O. J. Kleppa. *Enthalpies of Formation of Borides of Iron, Cobalt, and Nickel by solution calorimetry in liquid Copper*. Metallurgical Transactions B 13B, 251 (1982).

[24] E. Koch, W. Fischer. *DIDO95 and VOID95 – programs for the calculation of Dirichlet domains and coordination polyhedral*. Zeitschrift fur Kristallographie 211, 251 (1996).

[25] NIST Inorganic Crystal Structure Database (ICSD), NIST Standard Reference Database Number 3, collection code 613424. National Institute of Standards and Technology, Gaithersburg MD, 20899, DOI: https://doi.org/10.18434/M32147 (retrieved 2018)

[26] K. Saito, S. Doi, T. Abe, K. Ono, Quantitative evaluation of site preference in Dy-substituted $Nd_2Fe_{14}B$. J. of Alloys Compd. 721, 476 (2017)

[27] C. Skelland, T. Ostler, C. Westmoreland, *et al.*. *Probability distribution of substituted Titanium in RT_{12} (R = Nd and Sm; T = Fe and Co) Structures*. IEEE Trans. Mag. 54, 2103405 (2018).